

Detection of heavy metals (Cu^{+2} , Hg^{+2}) by biosynthesized silver nanoparticles

Swarnali Maiti¹ · Gadadhar Barman¹ · Jayasree Konar Laha¹

Received: 17 March 2015 / Accepted: 21 April 2015 / Published online: 23 May 2015
© The Author(s) 2015. This article is published with open access at Springerlink.com

Abstract Here, we are reporting two methods for detection of Cu^{+2} ion and Hg^{+2} ions using biosynthesized silver nanoparticles. The detection of Cu^{+2} ion was based on changes in absorbance resulting from complex formation of the metal ion. Various concentrations of Cu^{+2} ion were used to test the linearity and sensitivity of the method. A new peak at around 770 nm, in addition to the peak of the AgNP at 406 nm, was observed in each case (above 20 μM). With the increase of concentration of Cu^{+2} ion solution, the absorbance at 406 nm peak decreased and that of 770 nm increased gradually. The calibration curve obtained from the ratio of the absorption coefficients of these two peaks ($E_{x770/406}$) versus concentration of Cu^{+2} ions enables one to estimate quantitatively the amount of Cu^{+2} ions present in water in μM levels. This AgNP was further functionalized with 3-mercapto-1, 2-propanediol (MPD) for detection of Hg^{+2} present in water by colorimetric method. As soon as Hg^{+2} solution was added in MPD-functionalized AgNP (MPD-AgNP), a new peak at around 606 nm appeared along with the peak at 404 nm. The new peak might be due to the aggregations occurred by the recognition of heavy metal ion Hg^{+2} by MPD-AgNP through dipropionate ion. A calibration curve between the ratios of the absorption coefficients of these two peaks ($E_{x404/606}$) and concentration of Hg^{+2} was drawn for quantitative estimation of Hg^{+2} present in water at μM level.

Keywords Silver Nanoparticles · *Citrullus lanatus* · Detection of Cu^{+2} and Hg^{+2} · Calibration curve

Introduction

Monitoring the levels of potentially toxic metal ions such as Cu^{+2} , Hg^{+2} in aquatic ecosystems is important because these ions can have severe effects on human health and the environment (Campbell et al. 2003). Copper is a transition metal which plays significant roles in environmental and biological systems. It is widely used in the industrial and agricultural sectors, but it is also highly toxic to organisms, such as algae, fungi and many bacteria and viruses (Merian 1991). High concentrations of copper in drinking water are hazardous to human health (Barranguet et al. 2003). Some cases of liver damage of children have been proved to be associated with the excessive intake of copper (Zietz et al. 2003). Moreover, high concentrations of copper may destroy the biological reprocessing systems in water (Zhao et al. 2009). Mercury-based pollutants that arise mainly from coal-burning power plants are of great environmental concern because of high toxicity of many Hg compounds (Wang et al. 2004). Hg^{+2} is one of the most toxic metal ion and damages various human organs (Zahir et al. 2005; Zheng et al. 2003), resulting in serious symptoms and health deterioration. Therefore, the fabrications of sensitive and selective methods to monitor the presence of Cu^{+2} ions as well as Hg^{+2} are of great significance to protect public health and environment.

Many methods for detection of Cu^{+2} and Hg^{+2} ions have been reported till date. Most of them include chromogenic sensors (Banthia and Samanta 2005), Chemodosimeter-functionalized sensor (Kim et al. 2008a, b), fluorescent chemosensor (Zhang et al. 2011), atomic absorption spectroscopy (Gonzales et al. 2009), inductively coupled plasma

✉ Jayasree Konar Laha
j.laha@yahoo.co.in

¹ Department of Chemistry, Midnapore College, Midnapore
721101, West Bengal, India

mass spectroscopy (Backer et al. 2005) and inductively coupled plasma atomic emission spectroscopy (Liu et al. 2005) for detection of Cu^{+2} ions. Chemical sensors for the detection of Hg^{+2} include devices based on thin films of gold (Morris and Szulczewski 2002), polymeric materials (Tang et al. 2006), bio-composites (Ono and Togashi 2004), Chemodosimeter-functionalized sensor (Lee et al. 2009) etc. There is still a scope to develop new practical assays for determining Cu^{+2} and Hg^{+2} in real samples. In recent years, gold and silver nanoparticles have been widely used as colorimetric probes for chemical sensing and biosensing of various substances (Zhao et al. 2008) such as viruses (Niikura et al. 2009), cancerous cells (Midley et al. 2008), toxins (Uzawa et al. 2008), heavy metals (Barman et al. 2014a, b; Fan et al. 2009), pesticides (Barman et al. 2013; Maiti et al. 2013; Dasary et al. 2009), many inorganic and organic pollutants in water (Daniel et al. 2009; Xiao and Yu 2010). The methods of determination rely on their unique size and interparticle distance-dependent absorption spectra and color change of the solution. Inspired by the outcome of the abovementioned methods, we attempted a colorimetric application for detection of toxic metals like Cu^{+2} and Hg^{+2} ions in the solution. In this work, the synthesis of silver nanoparticles has been carried out using the juice extract of *Citrullus lanatus* (watermelon). The *Citrullus lanatus* is a good source of vitamin A and C. The presence of polyphenol in this juice is found to be responsible for the reduction of Ag^{+1} to Ag^0 ions and also stabilization of AgNP (Maiti et al. 2014; Huang et al. 2010; Prakash and Prakash 2011).

Experimental

Chemicals

Silver nitrate, AR grade, was purchased from Sigma-Aldrich Chemical Ltd. Sodium hydroxide and 3-mercaptopropylamine

1, 2-propanediol were purchased from Merck. The metal salt $\text{Cu}(\text{NO}_3)_2$ and $\text{Hg}(\text{NO}_3)_2$ were purchased from Beijing Chemical Reagent Company (Beijing, China). Double distilled de-ionized water was used in all experiments.

Preparation of juice extract

The *Citrullus lanatus* was collected from local market and washed with Double distilled de-ionized water. It was cut into pieces. The inner red portion of the pieces was pased by mortar pestle. Then, it was filtered using whatman filter paper to get *Citrullus lanatus* juice.

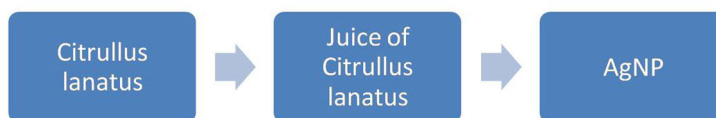
Synthesis of silver nanoparticles

Five milliliter of double distilled de-ionized water was added to 5 ml of pure juice extract to make it 1:1 and it was cooled in ice cold water. The solution was made alkaline (pH 10) by adding NaOH. The whole apparatus was placed on a heating mantle. During heating 6 ml 3×10^{-3} (M) aqueous silver nitrate solution was added drop wise with continuous stirring from burette and finally it was heated for 20 min at 70 °C. The color of the solution gradually changed from light pink to reddish yellow. The reddish yellow color indicated the formation of AgNP (Scheme 1).

Detection of Cu^{+2} by sensing the colorimetric property of AgNP

The colorimetric detection of aqueous Cu^{+2} ion was studied using AgNP solution at room temperature. To demonstrate the effect of Cu^{+2} ion on AgNP, 500 μL portions of several concentrations of Cu^{+2} ion (0–200 μM) were added one at a time to 3 ml of AgNP and the resulting mixture was then allowed to stand for 10 min at room temperature, during which the yellow color changed to

Scheme 1 Photographic images of *Citrullus lanatus*, its juice and silver nanoparticle



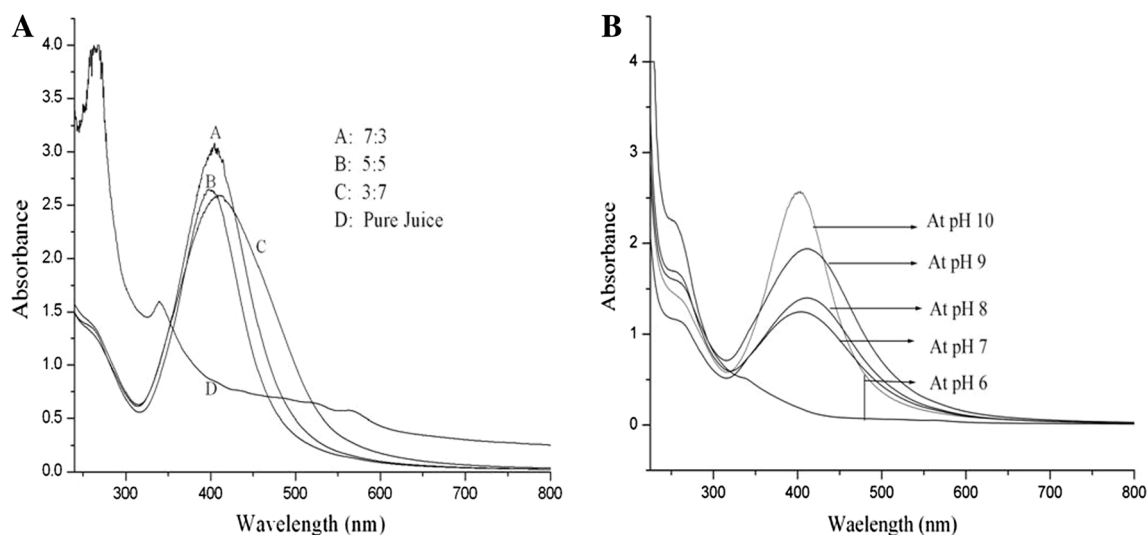


Fig. 1 UV-Vis spectra of **A** AgNP at different compositions of *Citrullus lanatus* juice extract and **B** AgNP at different pH

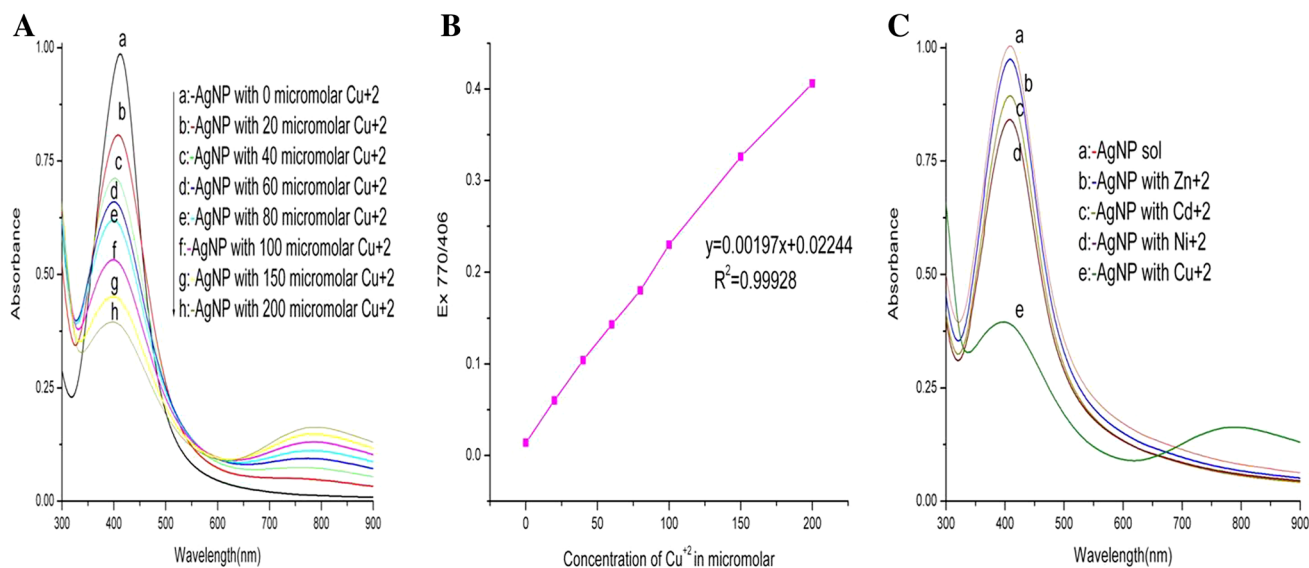


Fig. 2 UV-Vis spectra of **A** AgNP at varying concentrations of Cu^{+2} ion **B** Calibration curves between absorption ratios ($\text{Ex}_{770/406}$) versus concentration of Cu^{+2} ion **C** specificity of the proposed assay for the detection of Cu^{+2} against other metal ions

bluish. The intensity of this color gradually increased with the increase of Cu^{+2} ion concentration.

Detection of Hg^{+2} by sensing the Colorimetric property of functionalized AgNP

One ml 3×10^{-3} (M) 3-mercapto-1, 2-propanediol (MPD) was added to alkaline (pH10) 10 ml of as prepared AgNP sol to form MPD-functionalized AgNP (MPD-AgNP). This was used for detection of Hg^{+2} ions in water. Various concentrations of $\text{Hg}(\text{NO}_3)_2$ (0–600 μM) were prepared from stock solution by quantitative dilution. The colorimetric detection of Hg^{+2} in aqueous solution was studied at

room temperature. Typically, 3 ml of MPD-AgNP solution was added to 100 μl of $\text{Hg}(\text{NO}_3)_2$ solutions of different concentrations with continuous stirring and thereby the yellow color subsequently changed to blackish.

Characterization

The absorbance spectra of the AgNP were analyzed using a ‘SHIMADZU’ UV 1800 spectrophotometer and TEM images were taken using JEOL-JEM 2100 high-resolution transmission electron microscope (HRTEM). Samples for the TEM studies were prepared by placing a drop of the aqueous suspension of particles on carbon-coated copper

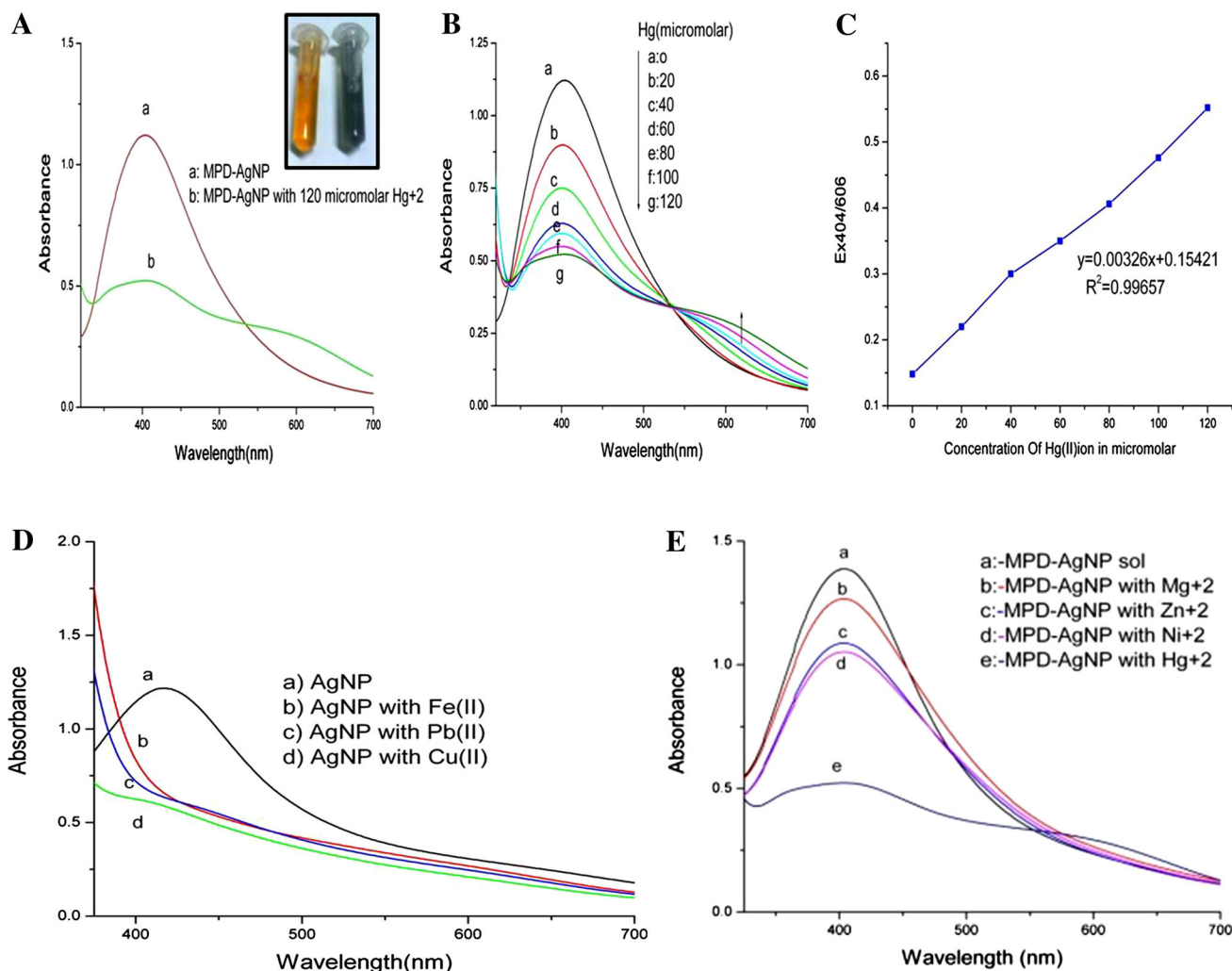


Fig. 3 UV-Vis spectra of **A** a MPD-AgNP and b MPD-AgNP with 120 μM Hg^{+2} **B** UV-Vis spectra of functionalized AgNP at varying concentrations of Hg^{+2} (0–120 μM) **C** Calibration curves between

absorption ratios (Ex 404/606) versus concentrations of Hg^{+2} (0–120 μM). **D**, **E** MPD-AgNP with various metals having concentration of 120 μM

grids followed by solvent evaporation under vacuum. The crystalline nature of the AgNP was examined using X' Pert Pro X-ray diffractometer operated at a voltage of 40 kV and a current of 30 mA with Cu $K\alpha$ radiation. FTIR measurements of AgNP and copper complex of AgNP were studied by Perkin Elmer Spectrum Version spectrophotometer.

Results and discussion

UV-Vis spectral studies

Optimization of synthesized AgNP

In the present work, the *Citrullus lanatus* juice extract was utilized for the synthesis of silver nanoparticles. For the

preparation, we have tried three different compositions (extract:water) at pH 10. For 3:7 ratios, a broad absorption band was observed at 410 nm and a sharp but not smooth curve found in case of 7:3 composition at 406 nm. The Plasmon band appeared sharp and smooth at 406 nm when 5:5 composition was used (Fig. 1A). As the sharp, single peak represents the monodispersity of the sol, 5:5 (extract: water) composition was preferred by us. To investigate the effect of pH on the formation of AgNP, pH was varied by controlling the amount of NaOH. 5:5 composition extract having different pH was further tried for synthesis of AgNP. It was found that only at pH 10, a narrow and sharp peak was obtained with higher extinction coefficient. With the decrease of pH, the plasmon band gradually broadened with lower extinction coefficient. The sol was not formed at all at below pH 7 (Fig. 1B).

Fig. 4 TEM micrographs of AgNP (A, B) and SAED (C) image from (B)

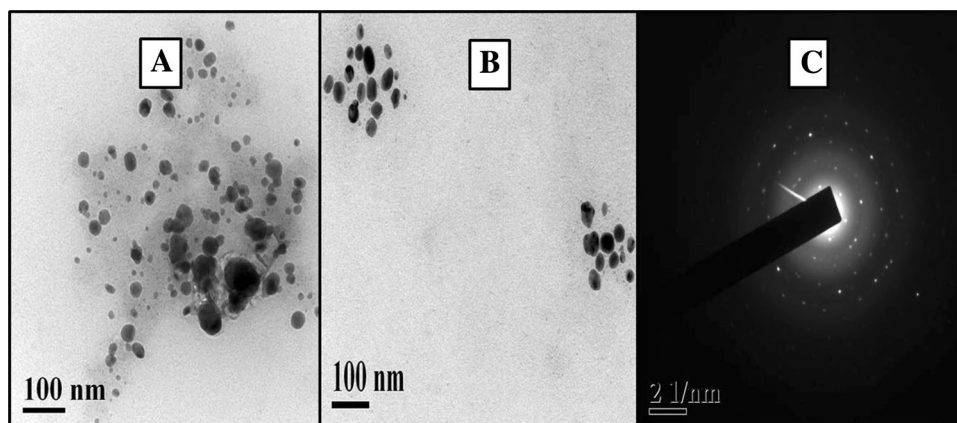
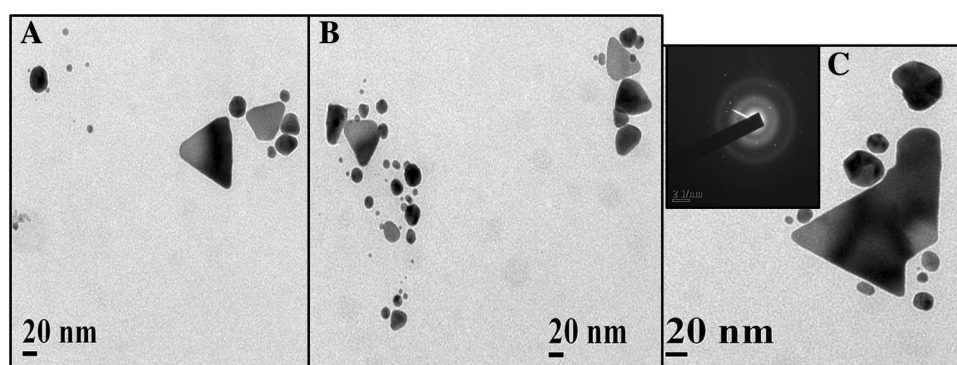
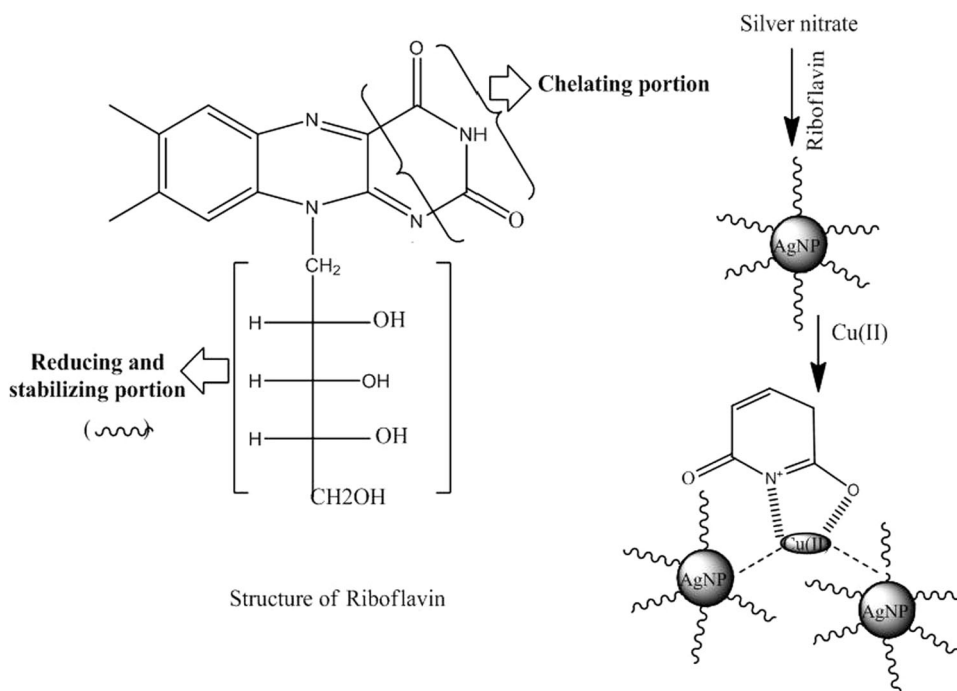


Fig. 5 TEM micrographs of Cu-complex with AgNP (A, B, C) and SAED image (inset of C) from C



Scheme 2 Probable schematic representation of stabilization AgNP and formation of coordination complex with Cu (II) ion

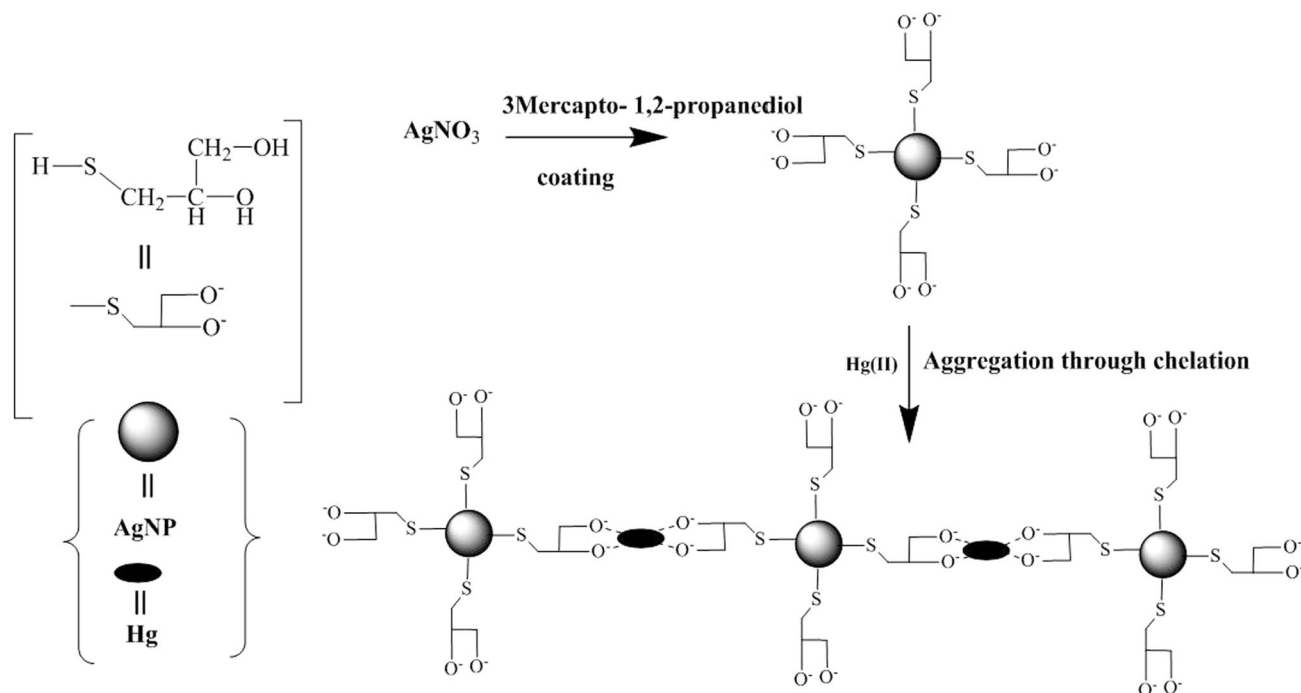
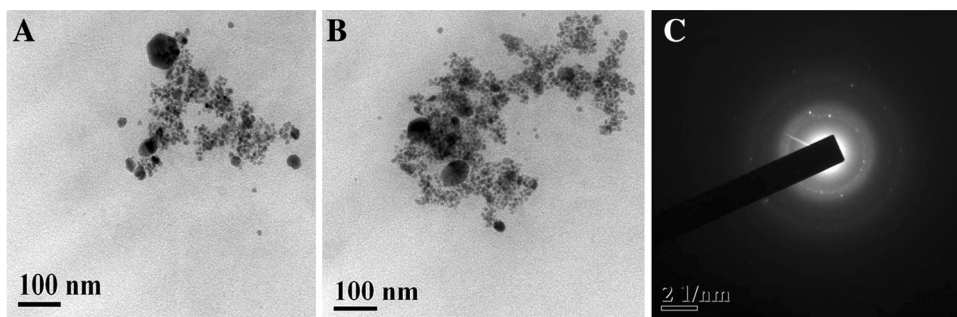


Detection of Cu^{+2} by sensing the colorimetric property of AgNP

For detection of Cu^{+2} ion present in aqueous solution, coordination complex formation method has been tried and

consequent color changes have been noticed. Several concentrations (0–200 μM) of $\text{Cu}(\text{NO}_3)_2$ solutions were used for the purpose of complex formation. Different concentrations of Cu (II) solution were added one at a time to the AgNP solution and corresponding changes of the

Fig. 6 A, B MPD-AgNP with $120 \mu\text{M Hg}^{+2}$ and (C): SAED image from B



Scheme 3 Schematic representation of Chelation of Hg(II) ion

absorption coefficients were noted. In each case (above $20 \mu\text{M}$), we found a new peak at around 770 nm in addition to the peak of the AgNP. More interestingly, with the increase of concentration of Cu^{+2} ion solution, the absorbance of 406 nm peak decreased and that of 770 nm peak increased gradually (Fig. 2A). The change of the UV–Visible absorbance ratios ($\text{Ex}_{770/406}$) was found to be linear with the concentration of Cu^{+2} ion. The calibration curve obtained from this ratio of the absorption coefficients of these two peaks ($\text{Ex}_{770/406}$) versus concentration of Cu^{+2} ions enables one to estimate quantitatively the amount of Cu^{+2} ions present in water in μM levels (Fig. 2B). Riboflavin, present in *Citrullus lanatus* Juice, contains polyphenol which might be responsible for the stabilization of AgNP. (Huang et al. 2010; Prakash and Prakash 2011) and the peptide linkage ($-\text{CONH}-$) for formation of coordination complex with Cu^{+2} (Garland 1973; Szilágyi et al. 2005).

The formation of the complex is evidenced from the color change (detectable by human eye) and the appearance of a peak at around 770 nm (Barman et al. 2014a, b; Li et al. 2013; Frederix et al. 2003). We repeated the experiment taking other heavy metal ions like Fe^{+2} , Pb^{+2} , Hg^{+2} , Zn^{+2} , Cd^{+2} , Ni^{+2} one at a time in place of Cu^{+2} ion. Fe^{+2} , Pb^{+2} and Hg^{+2} destroyed the sol completely whereas in case of Zn^{+2} , Cd^{+2} , Ni^{+2} , though no precipitation occurred, but they could not produce any significant color change and thus no change in the UV–Visible absorption spectrum (Fig. 2C). These findings tested the specificity of this assay for detection of Cu^{+2} ion.

Detection and estimation of Hg^{+2} ions using MPD-AgNP

The detection of minimum concentration of Hg^{+2} in aqueous solutions by color changes has been performed by utilizing the chelating ability of MPD. Several

concentrations of $\text{Hg}(\text{NO}_3)_2$ solutions (20–120 μM) were added to MPD-functionalized AgNP and the corresponding changes of the absorption coefficient were observed. In presence of Hg^{+2} ion, a new peak at around 606 nm appeared (above 40 μM) in addition to the peak found at 404 nm and with the increase of the concentration of Hg^{+2} ion, the absorbance of the 606 nm peak increased and that of AgNP peak decreased gradually (Fig. 3B). This phenomenon suggested that with the increase of the concentration of Hg^{+2} ion, complex formation enhanced with MPD-AgNP might be through the O atom available in MPD. The absorption coefficient ratio (the ratio of the absorption coefficient of MPD-AgNP peak at 404 nm and peak of sol in presence of Hg^{+2} at 606 nm $\text{Ex}_{404/606}$) measured the changes in absorption peak explicitly by the addition of Hg^{+2} . The change in coefficient confirmed that the ratio increased with the increase of concentration of the Hg^{+2} . A calibration curve obtained from the ratio of the absorption coefficients of these two peaks ($\text{Ex}_{404/606}$) versus concentration of Hg^{+2} ion may be applicable to estimate the amount of Hg^{+2} present in water in μM level (up to 120 μM) (Fig. 3C).

The experiment was repeated using other heavy metal ions like Fe^{+2} , Cu^{+2} , Pb^{+2} , Mg^{+2} , Zn^{+2} and Ni^{+2} one at a time in place of Hg^{+2} (120 μM to 3 ml of MPD modified AgNP). For Fe^{+2} , Cu^{+2} , Pb^{+2} precipitation occurred (Fig. 3D) and Mg^{+2} , Zn^{+2} ; Ni^{+2} could not produce any significant change in color and UV–Visible spectrum (Fig. 3E) which suggested the specificity of this assay for detection of Hg^{+2} ions.

HRTEM analysis

Figures 4 and 5 are due to the TEM images of AgNP produced from *Citrullus lanatus* juice extract and the Cu-complex of AgNP, respectively. It was observed in Fig. 4 that the particles were mostly spherical and their sizes varied from 10 to 50 nm. Selected area diffraction (SAED) pattern illustrated the crystalline nature of AgNP (Fig. 4C).

Due to the coordination complex formation with Cu^{+2} ion, the morphology of the AgNP changes appreciably (Scheme 2) which is evident from the TEM micrographs (Fig. 5). Different morphologies such as hexagonal, triangular, and heptagonal, along with the spherical structures (Fig. 5) are visible. The formation of complex was further confirmed from the FTIR spectra.

Figure 6 shows the TEM images of Hg^{+2} complex with functionalized AgNP. The strong binding of the Hg^{+2} metal ions with the functionalized AgNP through the O atom of MPD facilitated the aggregation of the silver nanoparticles (Scheme 3) and hence polydispersed silver nanoparticles having various morphologies like hexagonal, tetrahedron or dumb bell shaped along with spherical

particles were observed which are shown in the TEM micrographs (Fig. 6A, B). Selected area diffraction (SAED) pattern illustrated the crystalline nature of the complex formed between MPD-AgNP and Hg^{+2} .

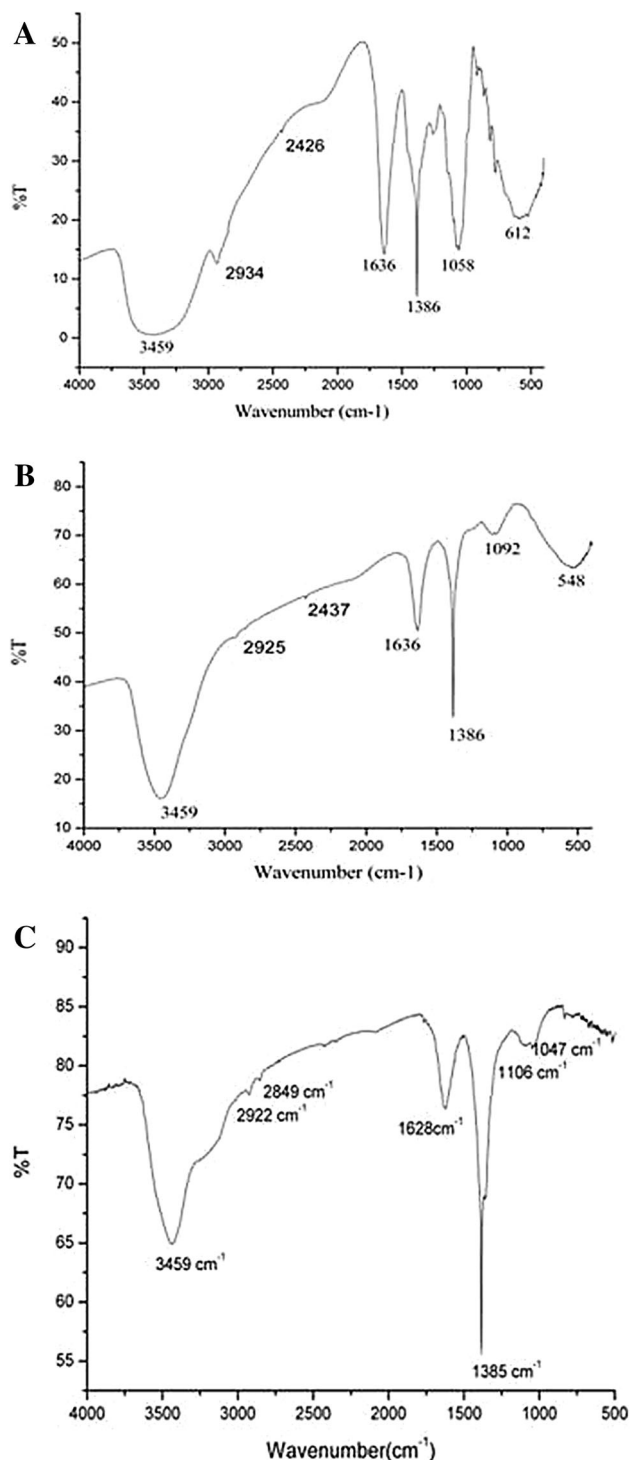


Fig. 7 FT-IR spectra of vacuum-dried powder of **A** *Citrullus lanatus* juice and **B** AgNP **C** AgNP complexed with Cu^{+2} ion

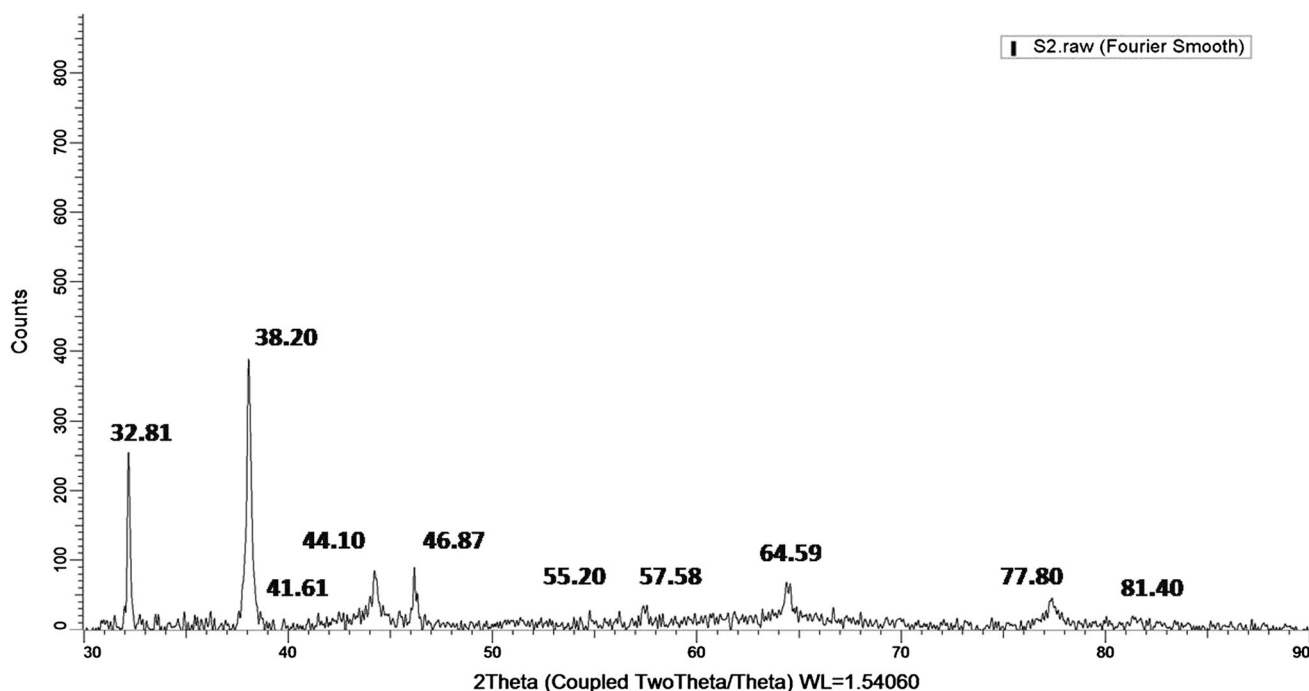


Fig. 8 XRD pattern copper complex of AgNP

FTIR analysis

Representative FTIR spectra of pure *Citrullus lanatus* juice and the synthesized AgNP are shown in Fig. 7A, B, respectively. The spectrum of *Citrullus lanatus* juice shows broad peak between 3300 and 3600 cm^{-1} which may be due to hydroxyl (OH) stretching bands of polyphenols present in riboflavin as well as NH bands present in peptide linkage (Renugadevi et al. 2010). AgNP spectrum shows slightly narrower peak in this region which suggests the involvement of the polyphenols (Song et al. 2009) in the reduction. The peak at 1636 cm^{-1} may be due to the presence of carbonyl group (C = O) associated with NH moiety in Riboflavin. When Cu^{+2} ion forms complex with modified AgNP the peak at 1636 cm^{-1} shifts to 1628 cm^{-1} (Fig. 7C). This shift indicates the involvement of peptide linkage present in Riboflavin during complex formation.

XRD analysis

The XRD analysis was performed to confirm the crystalline nature of the biosynthesized AgNP. The AgNP shows peaks at 38.20°, 44.10°, 64.59° and 77.80° which are found normally. The findings indicate that the synthesized AgNP is crystalline and essentially fcc in nature. XRD of the Copper complex of AgNP (Fig. 8) shows peaks at 32.81°, 41.61°, 46.87°, 55.20°, 57.58°, 81.84° in addition to the above peaks.

Conclusions

Here, we have reported methods for detection of Cu^{+2} ion and Hg^{+2} ions using biosynthesized silver nanoparticles. The detection of Cu^{+2} ion present in aqueous solution was based on changes in absorbance resulting from complex formation of the metal ion. Various concentrations of Cu^{+2} ion were tried to test the linearity and sensitivity of the method. A new peak at around 770 nm, in addition to the peak of the AgNP at 406 nm, was observed in each case (above 20 μM). With the increase of concentration of Cu^{+2} ion solution, the absorbance at 406 nm peak decreased and that of 770 nm increased gradually. The calibration curve obtained from the ratio of the absorption coefficients of these two peaks ($E_{x770/406}$) versus concentration of Cu^{+2} ions enables one to estimate quantitatively the amount of Cu^{+2} ions present in water in μM levels. This AgNP further functionalized with 3-mercapto-1, 2-propanediol for detection of Hg^{+2} present in water by colorimetric method. A new peak at around 606 nm appeared along with the peak of AgNP when solution of Hg^{+2} was added in functionalized AgNP (MPD-AgNP). The appearance of the peak might be due to the recognition of heavy metal ion Hg^{+2} by MPD-AgNP through dipropionate ion. A calibration curve between the ratios of the absorption coefficients of these two peaks ($E_{x404/606}$) and concentration of Hg^{+2} was exploited for quantitative estimation of Hg^{+2} present in water at μM level.

Acknowledgments We are thankful to Central Research Facility at IIT, Kharagpur, India for HRTEM and XRD studies.

Conflict of interest The authors declare that there is no competing interest.

Open Access This article is distributed under the terms of the Creative Commons Attribution 4.0 International License (<http://creativecommons.org/licenses/by/4.0/>), which permits unrestricted use, distribution, and reproduction in any medium, provided you give appropriate credit to the original author(s) and the source, provide a link to the Creative Commons license, and indicate if changes were made.

References

- Backer JS, Zoriy MV, Pickhardt C (2005) Quantitative imaging of selenium, copper and zinc in thin sections of biological tissues (slugs-genus arion) measured by laser ablation inductively coupled plasma mass spectrometry. *Anal Chem* 77:6074–6080
- Banthia S, Samanta A (2005) A two-dimensional chromogenic sensor as well as fluorescence inverter: selective detection of copper (II) in aqueous medium. *New J Chem* 29:1007–1010
- Barman G, Maiti S, Konar Laha J (2013) Bio-fabrication of gold nanoparticles using aqueous extract of Red Tomato and its use as a Colorimetric Sensor. *Nanoscale Res Lett* 8:181
- Barman G, Samanta A, Maiti S, Konar Laha J (2014a) Colorimetric assays for the Detection of Hg⁺² ions using functionalized gold and silver nanoparticles. *Adv Sci Foc* 2:1–7
- Barman G, Samanta A, Maiti S, Konar Laha J (2014b) Detection of Cu⁺² ion by the synthesis of Bio-mass-silver Nanoparticle Nanocomposite. *Int J Sci Eng Res* 5(6):1086–1097
- Barranguet C, Van Den Ende FP, Rutgers M, Breure AM, Greijdanus M, Sinke JJ, Admiraal W (2003) Copper-induced modifications of the trophic relations in riverine algal-bacterial biofilms. *Environ Toxicol Chem* 22(6):1340–1349
- Campbell LM, Dixon DG, Hecky RE (2003) A review of mercury in Lake Victoria, East Africa: implications for human and ecosystem health. *J Toxicol Environ Health B* 6(4):325–356
- Daniel WL, Han MS, Lee JS, Mirkin CA (2009) Colorimetric nitrite and nitrate detection with gold nanoparticles probes and kinetic end points. *J Am Chem Soc* 131:6362–6369
- Dasary SSR, Singh AK, Senapati D, Yu H, Ray PC (2009) Gold nanoparticle based label-free SERS probe for ultrasensitive and selective detection of Trinitrotoluene. *J Am Chem Soc* 131:13806–13812
- Fan YJ, Liu Z, Wang L, Zhang JH (2009) Synthesis of starch-stabilized Ag nanoparticles and Hg⁺² Recognition in aqueous media. *Nanoscale Res Lett* 4:1230–1235
- Frederix F, Friedt J, Choi K (2003) Biosensing based on light absorption of nanoscaled gold and silver particles. *Anal Chem* 75(24):6894–6900
- Garland WT, Fritchif CJ (1973) Metalloflavoprotein Models: the crystal structure of Bis (Riboflavin) Bis (Cupric Perchlorate) Dodecahydrate. *The J. of Biological Chemistry*. 249(7):2228–2234
- Gonzales APS, Firmino MA, Nomura CS, Rocha FRP, Oliveira PV, Gaubeur I (2009) Peat as natural solid-phase for copper preconcentration and determination in a multicommuted flow system coupled to flame atomic absorption spectrometry. *Anal Chimica Acta* 636(2):198–204 <http://www.intechopen.com/download/pdf/38600>
- Huang X, Wu H, Liao X, Shia B (2010) One-step, size-controlled synthesis of gold nanoparticles at room temperature using plant tannin. *Green Chem* 12:395–399
- Kim YR, Kim HJ, Kim JS, Kim H (2008a) Rhodamine-Based “Turn-On” Fluorescent Chemodosimeter for Cu(II) on ultrathin platinum films as molecular switches. *Adv Mat* 20:4428–4432
- Kim HJ, Lee SJ, Park SY, Jung JH, Kim JS (2008b) Detection of Cu^{II} by a Chemodosimeter-Functionalized Monolayer on Mesoporous Silica. *Adv Material* 20:3229–3234
- Lee MH, Lee SW, Kim SH, Kang C, Kim JS (2009) Nanomolar Hg(II) detection using Nile blue chemodosimeter in biological media. *Org Lett* 11:2101–2104
- Li F, Wang J, Lai Y, Wu C, Sun S, He Y, Ma H (2013) Ultrasensitive and selective detection of copper (II) ions by dicoated silver nanoparticle-based SERS probe. *Biosens Bioelectron* 39(1):82–87
- Liu Y, Liang P, Guo L (2005) Nanometer titanium di oxide immobilized on silica gel as sorbent for preconcentration of metal ions prior to their determination by inductively coupled plasma atom ice mission spectrometry. *Talanta*, <http://www.ccsenet.org/journal/index.php/ijc/article/download/18264/12828> doi:10.1016/j.talanta.2005.04.035
- Maiti S, Barman G, Konar Laha J (2013) Synthesis of silver nanoparticles having different morphologies and its application in estimation of chlorpyrifos. *Adv Sci Foc* 1(2):145–149
- Maiti S, Barman G, Konar Laha J (2014) Biosynthesized Gold nanoparticles as catalyst. *Int J Scient Eng Res* 5(7):1229–1230
- Merian E (1991) Metals and their compounds in the environment. VCH, Weinheim **893**
- Midley CD, Smith JE, Tang Z, Wu Y, Bamrungsap S, Tan WH (2008) Gold nanoparticle-based colorimetric assay for the direct detection of cancerous cells. *Anal Chem* 80:1067–1072
- Morris T, Szulcowski G (2002) A spectroscopic ellipsometry, surface plasmon resonance and x-ray photoelectron spectroscopy study of Hg adsorption on gold surfaces. *Langmuir* 18:2260–2264
- Niikura K, Nagakawa K, Ohtake N, Suzuki T, Matsuo Y, Sawa H (2009) Gold nanoparticle arrangement on viral particles through carbohydrate recognition: a non-cross-linking approach to optical virus detection. *Bioconjugate Chem* 20:1848–1852
- Ono A, Togashi H (2004) Highly selective oligonucleotide-based sensor for mercury (II) in aqueous solutions. *Angew Chem Int Ed* 43:4300–4302
- Prakash CVS, Prakash I (2011) Bioactive chemical constituents from pomegranate (*Punica granatum*) juice, seed and peel—a review. *Int J Res Chem Environ* 1:1–18
- Renugadevi TS, Gayathri S (2010) *Int. J. pharm. Sci. Rev. Res.* 2:106
- Song JY, Jang HK, Kim BS (2009) Biological synthesis of gold nanoparticles using *Magnolia kobus* and *Diospyros kaki* leaf extracts. *Process Biochem* 44(10):1133–1138
- Szilágyi I, Labádi I, Hernádi K, Pálkó I, Nagy NV, Korecz L, Rockenbauer A, Kele Z, Kiss T (2005) Speciation study of an imidazolate-bridged copper (II)–zinc (II) complex in aqueous solution. *J Inorg Biochem* 99(8):1619–1629
- Tang Y, He F, Yu M, Feng F, An L, Sun H, Wang S, Li Y, Zhu D (2006) A reversible and highly selective fluorescent sensor for mercury (II) using poly (thiophene)s that contain thymine moieties *Macromol. Rapid Commun.* 27:389–392
- Uzawa H, Ohga K, Shinozaki Y, Ohsawa I, Nagatsuka T, Seto Y, Nishida Y (2008) A novel sugar- probe biosensor for the deadly plant proteinous toxin, ricin. *Biosens Bioelectron* 24:923–927
- Wang Q, Kim D, Dionysiou DD, Sorial GA, Timberlake D (2004) Sources and remediation for mercury contamination in aquatic systems—a literature review. *Environ Pollut* 131(2):323–336

- Xiao N, Yu C (2010) Rapid-response and highly sensitive non-cross linking colorimetric nitrite sensor using 4-aminothiophenol modified gold nanorods. *Anal Chem* 82:3659–3663
- Zahir F, Rizwi SJ, Haq SK, Khan RH (2005) Low dose mercury toxicity and human health. *Environ Toxicol Pharmacol* 20(2):351–360
- Zhang JF, Park M, Ren WX, Kim Y, Kim SJ, Jung JH, Kim JS (2011) A pellet-type optical nanomaterial of silica-based naphthalimide-DPA-Cu(II) complexes: recyclable fluorescence detection of pyrophosphate. *Chem Commun* 47:3568–3570
- Zhao W, Brook MA, Li YF (2008) Design of gold nanoparticle-based colorimetric biosensor assays. *Chem Biochem* 9:2363–2371
- Zhao Y, Zhang XB, Han ZX, Qiao L, Li CY, Jian LX, Shen GL, Yu RQ (2009) Highly sensitive and Selective Colorimetric and Off-On Fluorescent Chemosensor for Cu^{+2} in aqueous solution and Living Cells. *Anal Chem* 81(16):7022–7030
- Zheng W, Aschner M, Ghersi-Egea JF (2003) Brain barrier systems: a new frontier in metal neurotoxicological research. *Toxicol Appl Pharmacol* 1:192
- Zietz BP, Dieter HH, Lakomek M, Schneider H, Keßler-Gaedtke B, Dunkelberg H (2003) Epidemiological investigation on Chronic copper toxicity to children exposed via the public drinking water supply. *Sci Total Environ* 302(1–3):127–144